JOURNAL OF GEOPHYSICAL RESEARCH, VOL. 94, NO. C5, PAGES 6159–6168, MAY 15, 1989

On the Origin of the Azores Current

BIRGIT KLEIN AND GEROLD SIEDLER

Institut für Meereskunde, Kiel, Federal Republic of Germany

The Azores Current, south of the Azores Archipelago, is part of the subtropical North Atlantic gyre. Using an international hydrographic data set, we analyze mean and seasonal geostrophic transport fields in the upper 800 m of the ocean in order to determine the origin of the Azores Current in the western basin and seasonal changes in the related flow. Geostrophic currents are obtained by using the method applied by Stramma (1984) in the eastern basin. The Azores Current is found to originate in the area of the Southwest Newfoundland Rise (Figure 10). In winter an almost uniform current connects this region of origin with the Azores Current, while a branching into two current bands is observed in summer, with the southern band forming a marked cyclonic loop. Within the upper 800 m, all of the transport in the northern band and about 70% of the transport in the southern band recirculates in the eastern basin. Additionally, expendable bathythermograph data from the Azores Current region indicate an increase of eddy potential energy from winter to summer.

INTRODUCTION

Part of the North Atlantic subtropical gyre (Figure 1) is found east of the Mid-Atlantic Ridge in the Canary Basin [*Armi and Stommel*, 1983; *Stramma*, 1984; *Olbers et al.*, 1985; *Maillard*, 1986; *Stramma and Siedler*, 1988]. It is well established that a jetlike current exists south of the Azores, the Azores Current, which provides the major portion of the upper ocean transport to the eastern basin recirculation [*Käse and Siedler*, 1982; *Gould*, 1985; *Käse et al.*, 1985; *Siedler et al.*, 1985; *Sy*, 1988]. Indications of such a marked eastward flow southeast of the Azores can be found in the early analysis of *Wüst* [1935]. The distribution of density and probable water movements at 200 m given in part of his Figure 47 is presented in our Figure 2. The origin of the Azores Current appears to be in the Gulf Stream system south of the Grand Banks. His map is suggestive of the existence of two current bands between the Azores Current and the Gulf Stream, with the northern band (e.g., $\sigma_t = 26.9$) forming an anticyclonic loop and the southern band (e.g., $\sigma_t = 26.7$) forming a cyclonic loop west of the Mid-Atlantic Ridge before reaching the anticyclonic part of the gyre in the eastern basin. The more recent β spiral analysis of the *Levitus* [1982] data set by *Olbers et al.* [1985] leads to a horizontal velocity field at 500 m depth which also includes the flow from the Gulf Stream to the Azores Current, although with a less marked cyclonic loop which is found farther west (Figure 1).

Knowledge of the spatial structure and the seasonal variations of the subtropical gyre is an important prerequisite for comparing observed flow fields with results from oceanic circulation models. It is the aim of this study to determine in more detail the mean horizontal structure of the geostrophic transport field between the Azores Current and its origin in the Gulf Stream, and to determine the seasonal variations of this field. An international hydrographic data set is edited and, following the method applied by *Stramma* [1984] in the eastern basin, is used to determine volume transports in the upper ocean. In addition, an international expendable bathythermograph (XBT) data set provides information on seasonal changes in eddy potential energy in the Azores region.

Copyright 1989 by the American Geophysical Union.

Paper number 88JC04324.
0148-0227/89/88JC-04324$05.00

DATA SET AND VELOCITY REFERENCE LEVEL

The hydrographic data for this study were obtained from the World Data Center A for oceanography (WODC). In order to exclude shelf water samples, only stations with data from deeper than 100 m were considered. Stations with dubious data, apparent from spikes or systematic deviations, were rejected. For the region 26°–50°N and 8°–56°W a total of 8240 stations were retained. Mean profiles of temperature, salinity, density, and dissolved oxygen were then computed for 116 squares (3° × 3°) in a subarea of the North Atlantic (see Figure 3). The depth intervals chosen for averaging were 2 m in the upper 100 m, 10 m in the layer of 100 m to 1500 m, and 50 m below 1500 m. The data were smoothed with a five-point moving average, corresponding to 10-m, 50-m, and 250-m intervals, respectively, in the three layers. This produced a stronger smoothing in the upper layers and weaker smoothing in the deep ocean where data scatter is small.

In addition to the hydrographic data set, we obtained all XBT records available at the WODC, which were then used to compute variations in vertical displacements of isotherm depth. We restricted this analysis to the smaller region of 30°–44°N, 20°–44°W, which is also shown in Figure 3. Because of the greater density of XBT data it was decided to perform this analysis over 2° × 2° squares. The data set was examined, and all profiles having spikes or systematic deviations were rejected. Finally, 5693 profiles were retained. The number of XBT casts available in each 2° × 2° square is given in Figure 4.

LEVEL OF NO MOTION

The selection of reference levels for determining geostrophic velocities and transports follows an approach by *Stramma* [1984]. He used *Defant*'s [1941] method combined with information on the advection of water masses, as identified by oxygen and salinity extrema, together with a mass conservation scheme developed by *Fiadeiro and Veronis* [1982, 1983] to discriminate between plausible and implausible reference depths. Geopotential differences between neighboring stations were computed from the mean

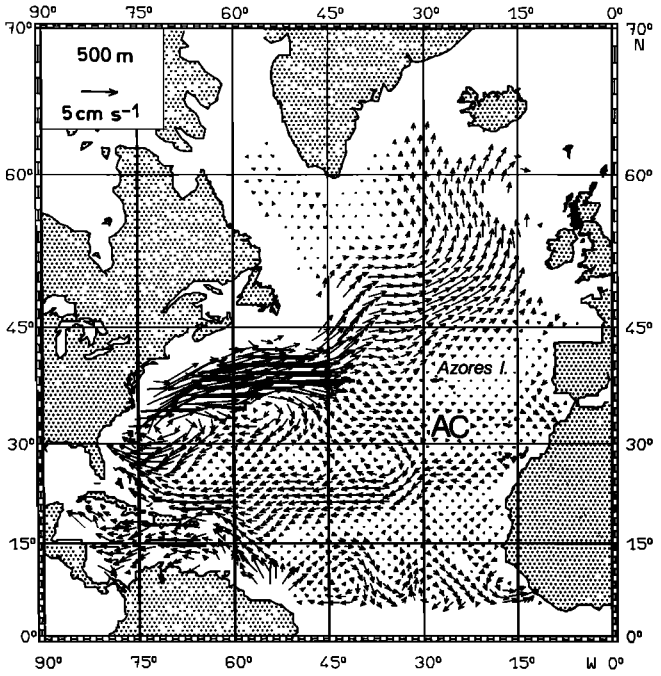

Fig. 1. Current at 500 m obtained from a β spiral analysis [after *Olbers et al.*, 1985]. The Azores Current is indicated by AC.

density profiles in each 3° × 3° square. Following Defant's method, possible reference depths are given by zero or small vertical gradients of geopotential anomaly differences. This method yields different possible reference depths. In order to eliminate unlikely levels, additional constraints were applied. It was demanded that a low vertical geopotential gradient should persist over more than 50 m and that low gradients should exist at nearly the same depths for neighboring geopotential profiles. In order to discriminate between the remaining levels, information about water mass spreading as inferred from mean temperature, salinity, and oxygen profiles for each 3° × 3° square was used. Distributions of salinity and oxygen extrema provided information about the spreading of Mediterranean Water, characterized by a salinity maximum, and Antarctic Intermediate Water, characterized by a salinity minimum. The oxygen minimum at about 800 m was an indicator of a slow-motion level. In addition to the above analysis we then used results from the Fiadeiro and Veronis mass conservation scheme in four selected subareas (Figure 5) to exclude unlikely levels. The method of Fiadeiro and Veronis is summarized, following *Stramma* [1984]:

Taking the density distributions on the boundaries of the closed subareas and using the equations of mass conservation, one can determine a likely reference depth for each volume. The criterion used to select the level is such that the minimum-mean-square transport imbalance for a set of mass-conserving, independent layers is obtained.

The hydrostatic and geostrophic balance yields the thermal wind relation:

$$\frac{\partial}{\partial z}\rho v = -\frac{g}{f}\frac{\partial \rho}{\partial x}$$

The velocity v_r, relative to the level z_r, where v is assumed to vanish is then obtained from

$$v_r = -\frac{g}{\rho f}\int_{z_r}^{z}\frac{\partial \rho}{\partial x}\,dz$$

The velocity field can be used to determine the mass flux within any layer between two stations. The total mass flux for the $j = 1, \cdots, F$ layers is given by

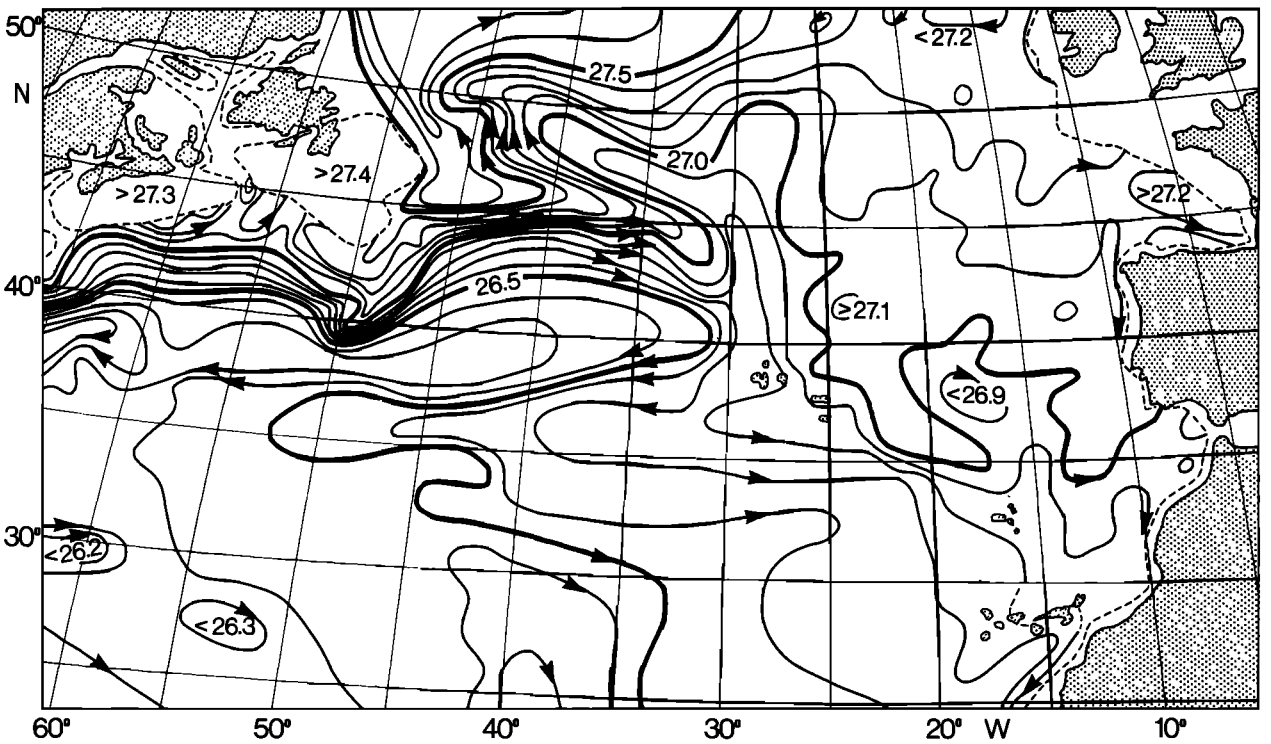

Fig. 2. Distribution of density σ_t at 200 m, with probable water movements indicated by arrows [after *Wüst*, 1935].

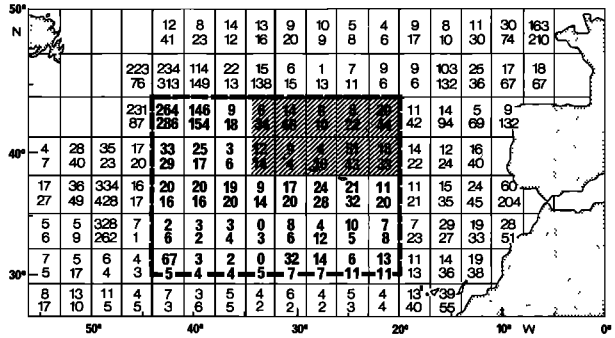

Fig. 3. Area of present analysis, with number of hydrographic stations indicated in each 3° × 3° square for the winter half year (above) and the summer half year (below). The eddy potential energy analysis using XBT data was performed in 2° × 2° squares in the central box; the 15°C isotherm was selected as representing upper thermocline variability, except in the hatched area, where the 13°C isotherm was used.

$$T_{rj} = \int_0^L \int_{z_{j+1}}^{z_j} \rho v_r \, dz \, dx$$

where z_j is the level of the top of the jth layer and L is the perimeter of the closed area. For data gridded at n discrete horizontal locations, $i = 1, \cdots, n$, the horizontal integral is approximated by a finite sum

$$T_{rj} = \sum_{i=1}^{n} \int_{z_{j+1}}^{z_j} \rho_i v_{ri} \, dz \Delta_i x$$

where $\Delta_i x = x_{i+1} - x_i$ ($\Delta_n x = x_1 - x_n$) and v_{ri} is evaluated at the midpoint $\Delta_i x$. The vertical integral v_{ri} and ρ_i are evaluated at 5-m intervals from 5 m to the bottom, and the vertical integral is also approximated by a discrete sum. Ideally, a level of no motion is found by varying z_r until T_{rj} vanishes. However, noise in the data and the possibility that no level of zero motion exists prevent T_{rj} from being exactly zero in practice. *Fiadeiro and Veronis* [1982] imposed the criterion that the mean-square transport residual

$$T_r^2 = \sum_{j=1}^{F} T_{rj}^2 = \min$$

is minimum at the level of no motion.

Following this description by *Stramma* [1984], in order to find layers where mass is most likely conserved, we examined fields of dissolved oxygen, salinity, potential density, and potential vorticity, using surfaces of constant potential density relative to 3000 dbar as boundaries between the layers. Four layers were selected (see Table 1). The resulting mean-square transport imbalances, ΣT_r^2, and the summation of net transport, ΣT_r, versus reference depths Z for the four subareas are shown in Figure 6. We draw the following conclusions for the four subareas:

Subarea A: This triangle in the subtropical region corresponds to subarea B of *Stramma* [1984]. Defant's method results in possible reference levels at 800 m and 1300 m. A minimum of ΣT_r^2 is found at 1200 m, with small values occurring below 2400 m. The ΣT_r has near-zero values between 1100 m and 2000 m and a zero crossing at 1540 m. The large transport imbalance in the upper 1000 m suggests that 800 m should not be chosen. We therefore selected 1300 m.

Subarea B: Defant's method results in possible reference levels at 900 m and around 1400 m. The minimum of ΣT_r^2 appeared together with a zero crossing of ΣT_r, near 1400 m depth. The sum of net transport, ΣT_r, is high in the upper layers and increases again below 1400 m. This led us to the rejection of the upper level and the selection of 1400 m.

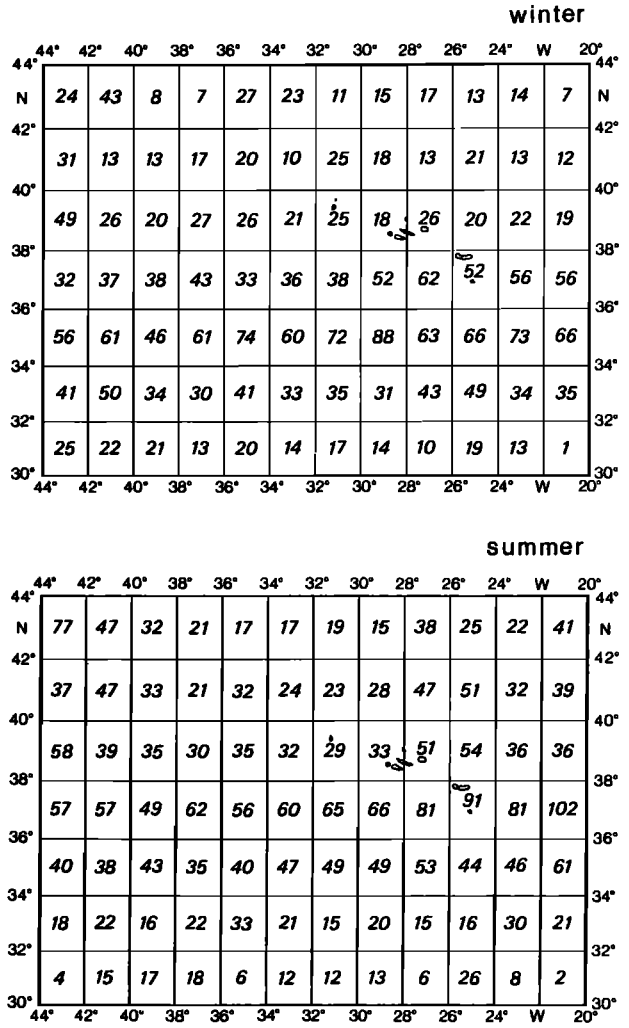

Fig. 4. Number of quality-checked XBT profiles available per 2° × 2° square for the winter and the summer half year.

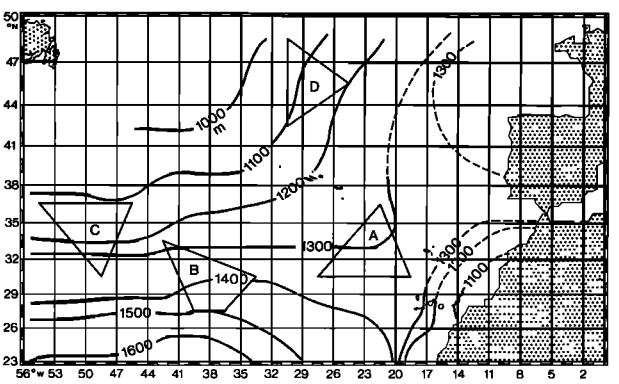

Fig. 5. Closed volumes A to D in which the mass conservation scheme was applied, and depth (meters) of the level of no motion obtained from this analysis.

TABLE 1. Potential-Density Interfaces (Relative to 3000 dbar) for the Subareas in Figure 5

Subarea A	Subarea B	Subarea C	Subarea D
surface	surface	surface	surface
40.50	40.20	40.53	41.02
41.26	41.31	41.32	41.28
41.48	41.41	41.45	41.37
bottom	bottom	bottom	bottom

Subarea C: Defant's method suggests possible reference levels of about 800 m and 1200 m. As in all other subareas, high values of ΣT_r and ΣT_r^2 were observed in the upper 800 m. In this case a zero crossing of ΣT_r appeared near 1200 m together with small values of ΣT_r^2. The shallower level was again rejected, and 1200 m was chosen.

Subarea D: This is the subarea which covers the northern part of the investigation area. Defant's method gives only one reference level: 1100 m. Here ΣT_r^2 is high in the upper layers and is small below 1100 m. The ΣT_r shows a zero crossing at 1100 m. Therefore the selected level was 1100 m.

Our selected reference levels in Figure 5 have the same spatial trend as found by *Stramma* [1984] but are somewhat deeper. Levels of no motion selected outside the closed volumes were those from Defant's method that most nearly coincided with those in the closed volumes. Because there are peculiarities in the Mediterranean outflow regime west of

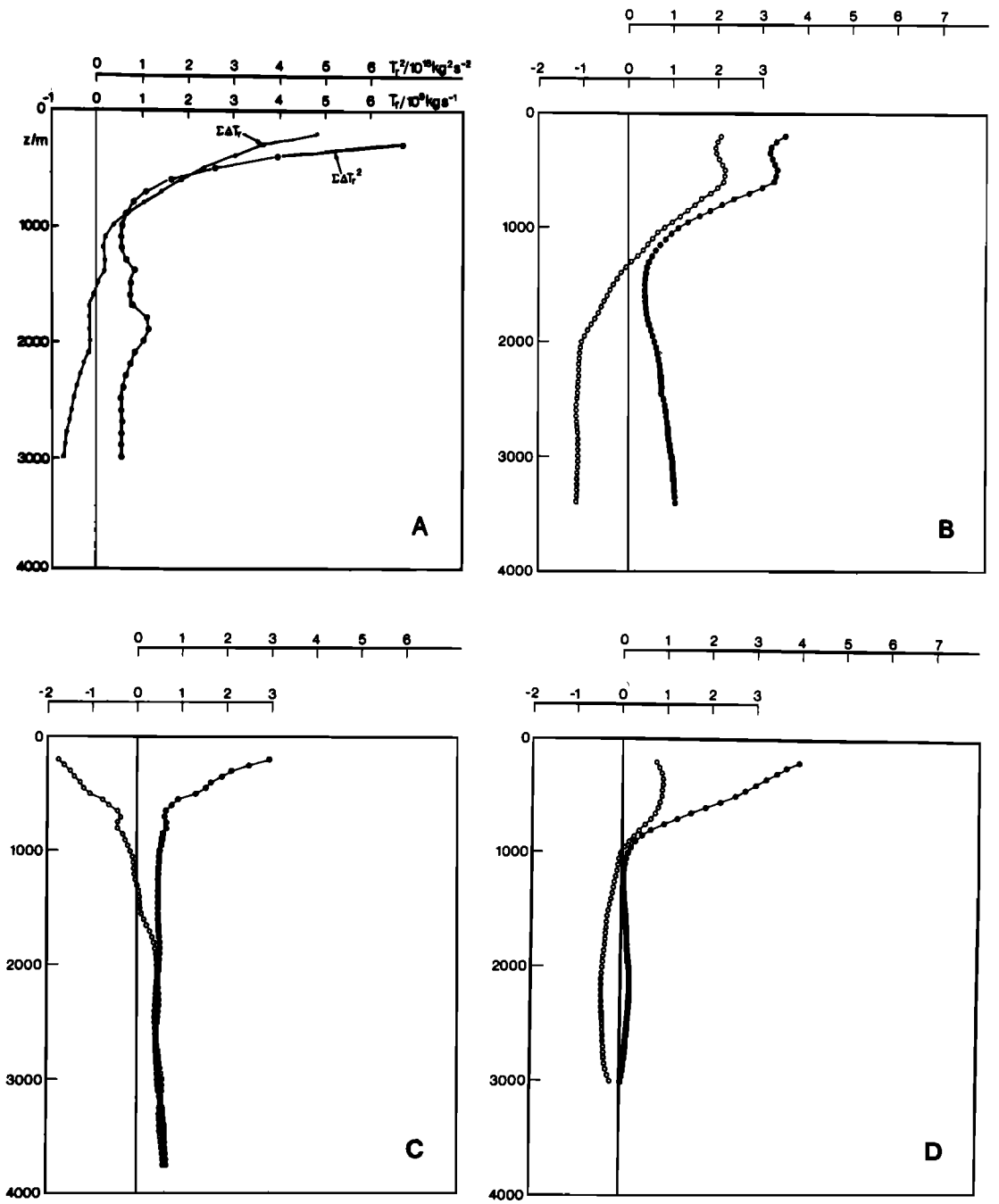

Fig. 6. Sum of transport imbalances T_r and mean-square transport imbalances T_r^2 versus reference depth z for the closed volumes A to D (see Figure 5).

Gibraltar, and also because this region is not considered in our analysis, we show the reference level depth there by dashed lines in Figure 5.

UPPER OCEAN GEOSTROPHIC TRANSPORTS

Geostrophic velocity components u (east) and v (north) were determined for the common corner point of four 3° × 3° squares by averaging the velocities across the square boundaries normal to the respective components on both sides of the corner point. Reference levels for zero velocity as described above were used to obtain velocity vectors and transports. The transport fields were obtained with objective analysis following the Gauss-Markov theorem. The correlation scale was selected as 450 km, representing approximately 1.5 times the meridional width of a 3° × 3° square used for spatial averaging. This ensures that the correlation scale is larger than the inherent scales of the eddy and meander field [*Fofonoff and Hendry*, 1985; *Krauss and Böning*, 1987]. A spatial trend was removed by two-dimensional regression before applying the objective analysis scheme. Volume transport fields were computed for the near-surface layer (0–200 m) and also for the upper ocean including the main thermocline (0–800 m). The total number of hydrographic stations available in each 3° × 3° square was given in Figure 3. The best data coverage is found near the eastern and western boundaries, with data being scarce in the center near the Mid-Atlantic Ridge. The areas southwest and southeast of the Azores are reasonably well covered. We concluded that the number of stations was not sufficiently large in several squares to obtain reliable information for all four seasons. The seasonal signal was therefore investigated by averaging over half-year periods. It can be expected that an average over December through May is dominated by typical oceanic winter conditions, while an average over June through November is dominated by oceanic summer conditions in this region. We therefore define the winter half year to be December–May and the summer half year to be June–November.

The annual and half-year mean transport streamline fields for 0–200 m are shown in Figure 7, and for 0–800 m in Figure 8. The increments between streamlines represent 1 Sv (10^6 m^3 s^{-1}) in Figure 7 and 1.5 Sv in Figure 8. The objective analysis provides an optimal interpolation procedure that minimizes the least squares error between data and fit. It also yields an estimate of the residual uncertainties in the interpolated values which depend on the statistics of the field, the noise level, and the locations of the observational points. These error fields are indicated, with errors larger than 0.5 Sv (Figure 7) or 1.0 Sv (Figure 8), by the dashed shading. The Azores Current is recognized in the annual mean flow field as an almost zonally oriented transport band south of the Azores, approximately between 32° and 36°N. Because of the meandering of the Azores front [*Gould*, 1985; *Käse et al.*, 1985], averaging and smoothing applied here produces a broader flow than has actually been observed in quasi-synoptic observations. The 0- to 800-m transport at 35°W is close to 10 Sv, which equals results from quasi-synoptic surveys [*Käse et al.*, 1986]. The 0- to 200-m layer contributes here 4 Sv.

In his earlier analysis, *Stramma* [1984] showed that the transports are not strongly affected by the use of deeper reference levels because of small variations of the current profiles below about 1000 m. He found that in most cases, transports between mean station pairs (3° × 3° squares) changed by less than 0.5×10^6 m^3 s^{-1} upon substitution of a 1000-m level by a 1500-m level of no motion. He also verified that the related potential vorticity fields did not change significantly when using a noise-simulating data set. We checked the significance of the computed transport patterns by varying the level of no motion with respect to the level given in Figure 5. In Figure 9 we show the example from a recomputation of the 0 to 800-m volume transport streamlines given in Figure 8, summer situation, where a 250-m shallower level and a 250-m deeper level of no motion was assumed. It appears that particularly in the region from the Newfoundland Rise to the Azores the pattern of the flow field is well preserved and that the main gyre transports change by less than 20%. This example demonstrates that the pattern of the transport field is sufficiently insensitive to errors in the determination of the level of no motion to permit the evaluation of the seasonal changes of this structure.

The source region of the Azores Current is found in the transition zone between the Gulf Stream and the North Atlantic Current in the area of the southeastern Newfoundland Rise. A division of the Gulf Stream into two branches in this region has long been recognized [*Iselin*, 1936], one branch flowing north across the rise and the other flowing east before it also divides into a northward and a southward branch, the latter recirculating into the Sargasso Sea. The source region of the Azores Current is also the area where *Worthington* [1962, 1976] proposed the existence of a separation into two independent anticyclonic gyres, an interpretation with which *Mann* [1967], *Mountain and Shuhy* [1980], and *Clarke et al.* [1980] disagreed. A review of this question was given by *Fofonoff* [1981]. More recent observations with surface drifters [*Richardson*, 1983] and SOFAR floats [*Owens*, 1984; *Schmitz*, 1985] give indications of a branching southeast of Newfoundland. *Krauss* [1986] presented an analysis based on *Dietrich et al.*'s [1975] results on the current system in the North Atlantic and trajectories from satellite-tracked drifting buoys and concluded that neither a permanent branching nor a confinement of the subpolar gyre to the east of Newfoundland can be found.

We are interested here in the part of the flow south and east of the Newfoundland Rise which connects the Gulf Stream system with the Azores Current. Following the flow from the region of origin, toward the Azores area, a cyclonic meander is found in the annual mean volume transport fields (Figures 7 and 8) in the neighborhood of 35°N, 41°W. A strong seasonal change is detected in this region. In the winter half year we find an almost uniform flow with the cyclonic meander in about the same place as in the annual mean fields. However, in the summer half year the flow separates into two current bands at about 41°N, 47°W. The northern band deviates only weakly from a direct path connecting the source region to the Azores Current, whereas the southern band forms a marked cyclonic loop 6° to 8° west of the winter meander around the Corner Seamounts (Figure 10). Contrary to what might be expected from *Worthington*'s [1976] conclusions, about 70% of the water in the southward flowing band (0–800 m) crosses the Mid-Atlantic Ridge into the eastern basin.

We find a branching into three major southward bands in the Canary Basin: just east of the Mid-Atlantic Ridge, in the central basin, and near the coast of western Africa. The

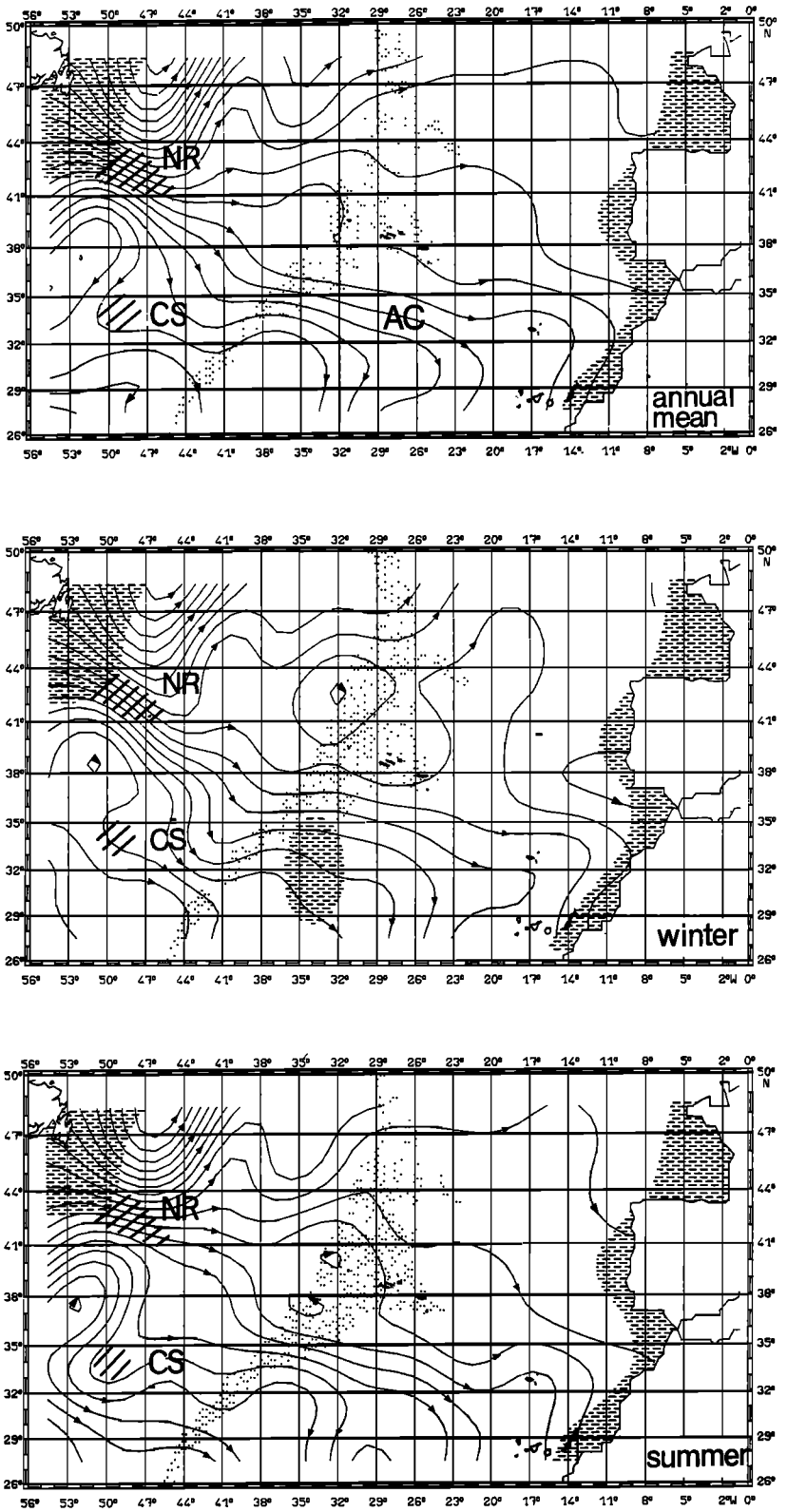

Fig. 7. Annual, winter half-year, and summer half-year mean volume transport streamlines in the layer 0–200 m. Increments between streamlines represent 1 Sv (10^6 m^3 s^{-1}). Error estimates are above 0.5 Sv in areas of dashed shading. Dotted stippling indicates position of Mid-Atlantic Ridge; heavy lines indicate Newfoundland Rise (NR) and Corner Seamounts (CS). The Azores Current is indicated by AC.

bifurcation of the Azores Current into the two easternmost bands has already been noted by *Stramma* [1984]. The Azores Current itself exhibits a seasonal change, with a shift of the zonal flow axis to the south in summer, which was discussed by *Stramma and Siedler* [1988]. They found a seasonal change in the structure of the subtropical gyre in the eastern North Atlantic, with a smaller north-south extension of the gyre in summer as compared to winter.

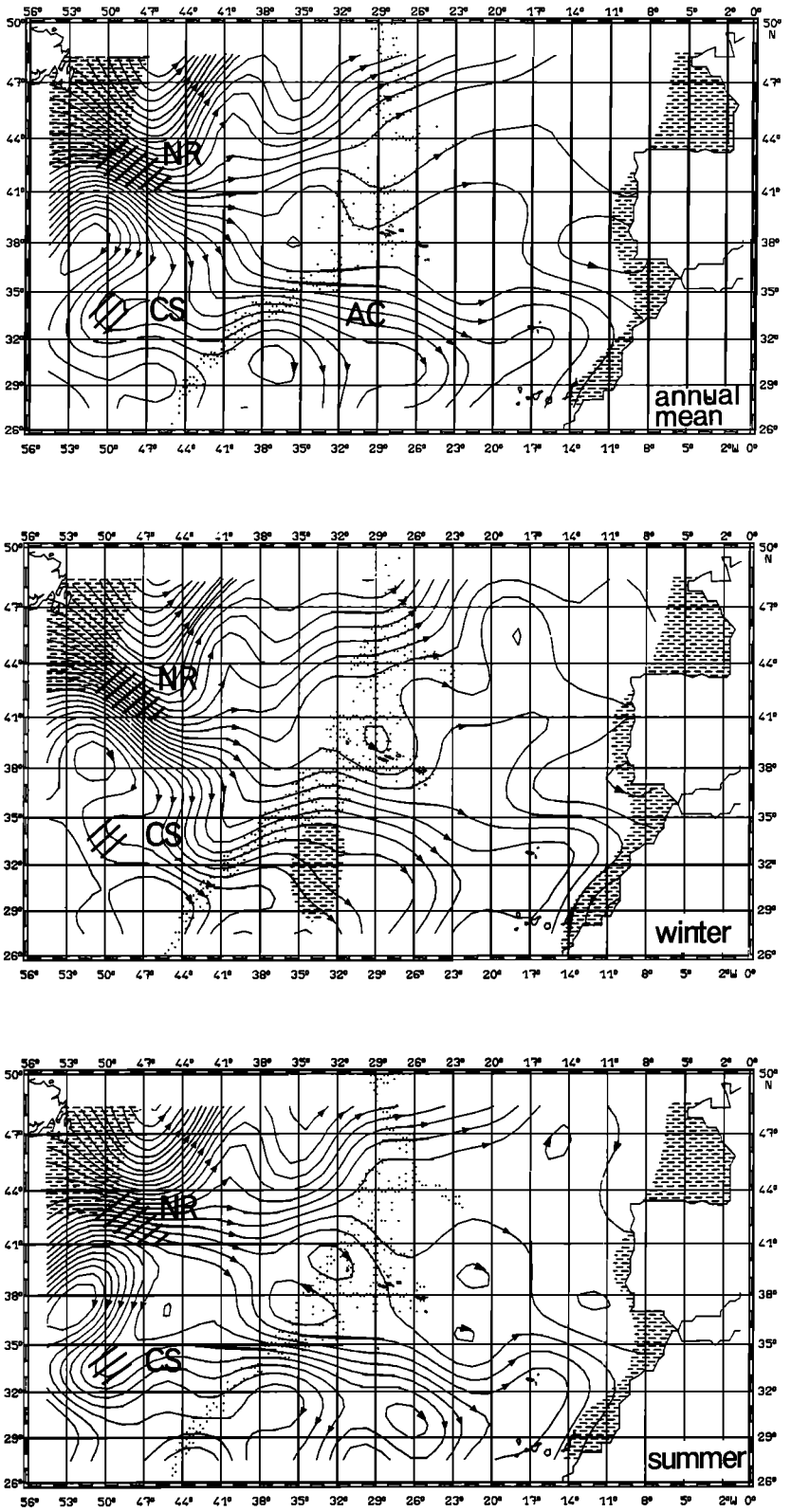

Fig. 8. Annual, winter half-year, and summer half-year mean volume transport streamlines in the layer 0–800 m. Increments between streamlines represent 1.5 Sv (1.5×10^6 m^3 s^{-1}). Error estimates are above 1.0 Sv in areas of dashed shading. Dotted stippling indicates position of Mid-Atlantic Ridge; heavy lines indicate Newfoundland Rise (NR) and Corner Seamounts (CS). The Azores Current is indicated by AC.

Seasonal Changes of the Eddy Potential Energy Field

The Azores Current seen in Figures 7 and 8 appears narrower in the summer half year than in the winter half year. This may be a result of reduced meandering then, or it might be due to a narrowing of the total flow with stronger horizontal gradients generated. In the first case, we expect reduced mesoscale temperature variability in the summer

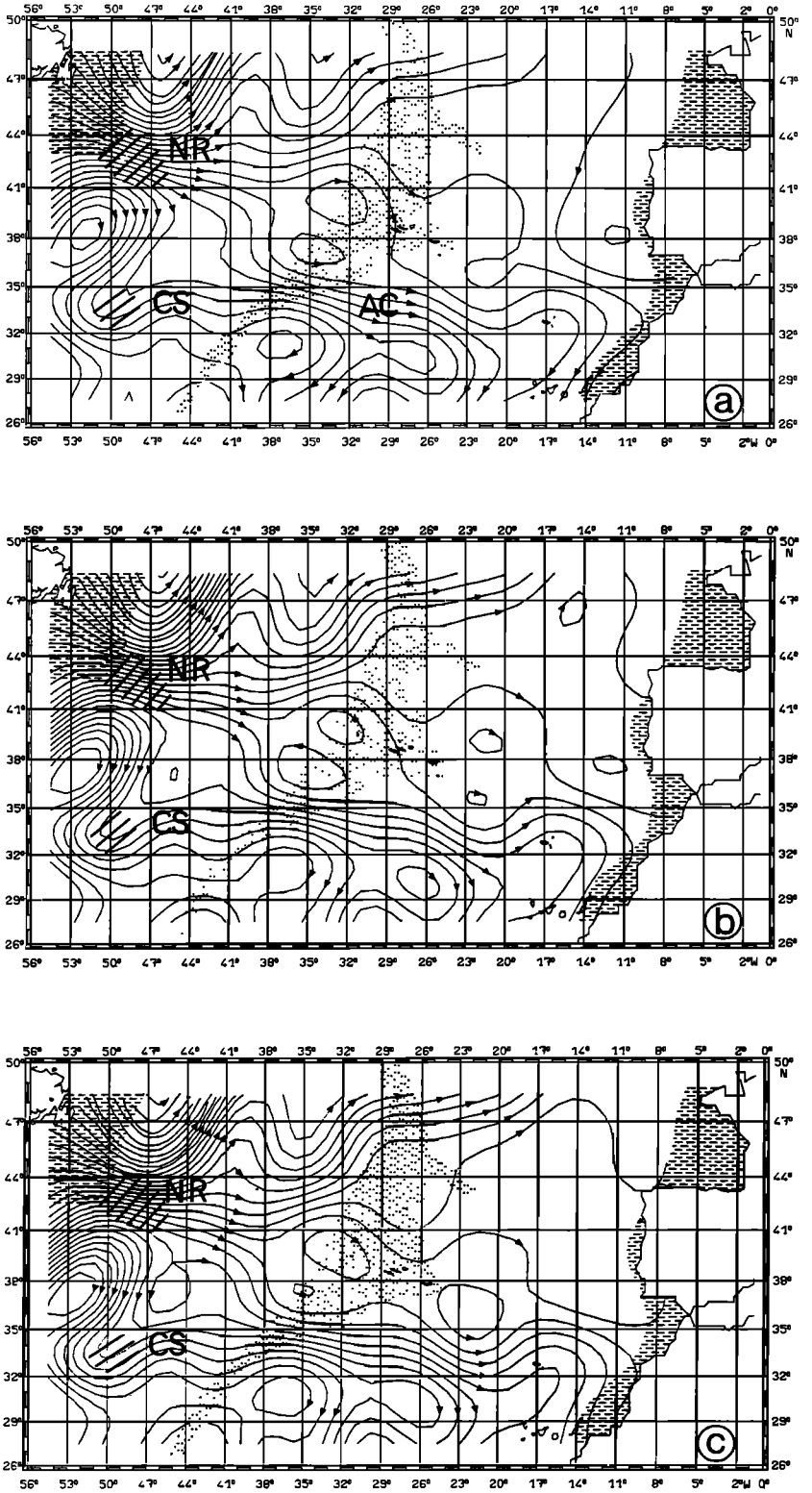

Fig. 9. Summer half-year mean volume transport streamlines in the layer 0–800 m for the case of (*a*) a 250-m shallower and (*c*) a 250-m deeper level of no motion than that given in Figure 5. (*b*) The transport field from Figure 8, summer situation, is repeated here for intercomparison. Increments between streamlines represent 1.5 Sv (1.5×10^6 m^3 s^{-1}). Dotted stippling indicates position of Mid-Atlantic Ridge; heavy lines indicate Newfoundland Rise (NR) and Corner Seamounts (CS). The Azores Current is indicated by AC.

thermocline owing to smaller horizontal displacements of water masses. In the second case, we expect greater mesoscale temperature variability from the fact that meandering of a flow has increased lateral temperature gradients. This can be checked by investigating the temperature variance, or rather the eddy potential energy (EPE), in the Azores Current region. We followed *Dantzler* [1977] in determining EPE = $0.5\overline{N^2\zeta^2}$, where N is the Brunt-Väisälä frequency and

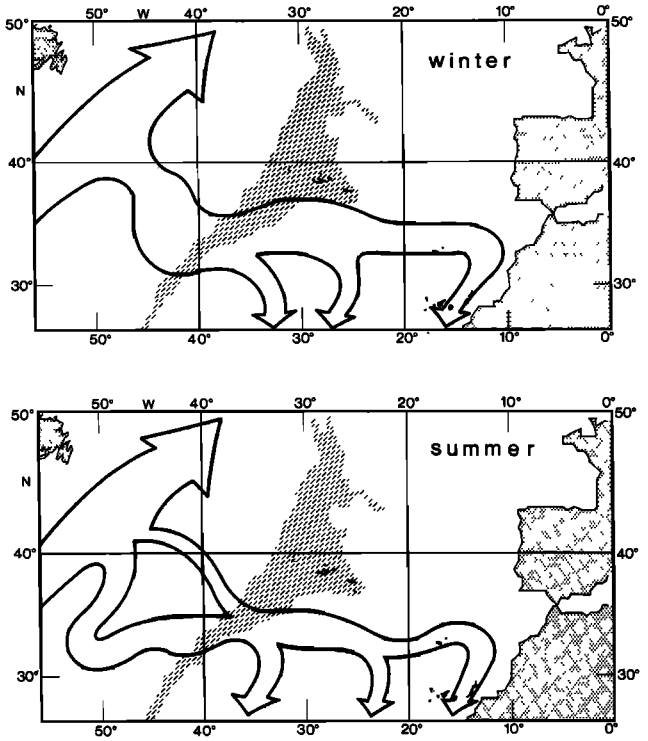

Fig. 10. Schematic presentation of the flow in winter and summer. Diagonally shaded areas indicate positions of Mid-Atlantic Ridge.

ζ is the vertical displacement of a selected isotherm from its mean depth in a 2° × 2° square. The subarea chosen for this analysis is indicated in Figure 3. The historical XBT data set previously described was used for determining ζ. The 15°C isotherm was used in most of the subarea to represent upper thermocline variability. In the area northeast of the Azores Archipelago the 13°C isotherm was selected instead, because the 15°C isotherm becomes shallow there and fluctuates with a strong seasonal signal. It was shown by *Emery* [1983] and by *Siedler and Stramma* [1983] that the variability of the mean temperature-salinity relationships in our area of study is sufficiently small in the main thermocline to allow the use of isotherms instead of isopycnals for the determination of potential energy changes.

$\overline{N^2}$ was obtained from the described hydrographic data set, but from annual averages over 2° × 2° squares in this case. Vertically averaged $\overline{N^2}$ values were determined between the depths of the 9°C and the 18°C isotherms (or the surface if colder than 18°C). The EPE field was analyzed by first subtracting a two-dimensional trend and then applying an objective analysis procedure with a correlation scale of 350 km, representing approximately 1.5 times the meridional width of a 2° × 2° square.

The results for the winter and the summer half years are presented in Figure 11. The general pattern is consistent with *Dantzler*'s [1977] findings that higher values of EPE occur closer to the Gulf Stream. We additionally find, however, an increase in EPE from the winter half year to the summer half year in the Azores Current region, the increase coinciding with a narrowing of the current band. Therefore the narrowing of the current in summer can probably be associated with a strengthening of lateral gradients, which in turn lead to increased mesoscale variability.

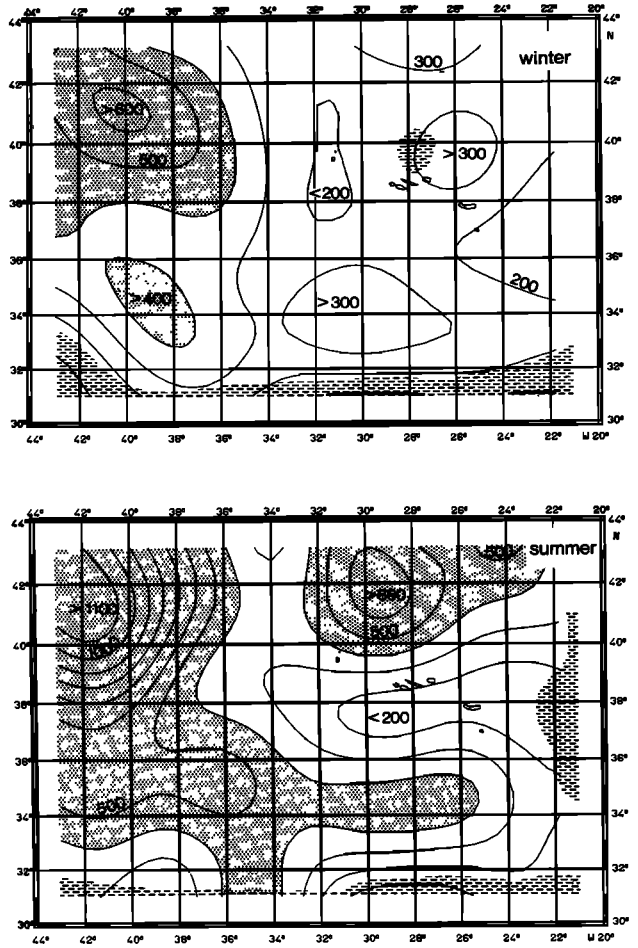

Fig. 11. Eddy potential energy in $cm^2\ s^{-2}$ in the area given in Figure 3 for the winter and the summer half year. Dotted stippling indicates levels above 400 $cm^2\ s^{-1}$. Error estimates are above 50% in areas with dashed shading.

CONCLUSIONS

The origin of the Azores Current is found to be in the transition region between the Gulf Stream and the North Atlantic Current near the southeastern Newfoundland Rise. It thus is an extension of the Gulf Stream system, an extension that displays a strong seasonal variability (Figure 10). In summer the flow from this source region separates into two bands, one flowing almost directly toward the Azores Current region and the second forming a marked cyclonic loop farther southwest before merging in the Azores Current. The generation of this loop in the south is probably related to topographic effects and seasonal changes in the wind stress curl. In the area under consideration the wind stress curl is near zero in winter and decreases to negative values in summer [*Isemer and Hasse*, 1985]. This could lead to a gyre return flow further west, while vorticity preservation would introduce a cyclonic motion around the Corner Seamounts area. The Azores Current narrows in summer and moves farther south, with increased eddy scale variability being found during this part of the year. The gyre recirculation in the Canary Basin has a three-banded structure, which is apparent during all portions of the year.

Acknowledgments. We would like to acknowledge the assistance of the data processing staff of the Marine Physics Group at the

Institut für Meereskunde, Kiel. The authors have benefited from discussions with L. Stramma, R. Käse, R. Onken, and R. G. Peterson. This study was supported by the Deutsche Forschungsgemeinschaft (SFB 133).

REFERENCES

Armi, L., and H. Stommel, Four views of a portion of the North Atlantic subtropical gyre, *J. Phys. Oceanogr., 13*, 828–857, 1983.

Clarke, R. A., H. W. Hill, R. F. Reiniger, and B. A. Warren, Current system south and east of the Grand Banks of Newfoundland, *J. Phys. Oceanogr., 10*, 25–65, 1980.

Dantzler, H. L., Potential energy maxima in the tropical and subtropical North Atlantic, *J. Phys. Oceanogr., 7*, 512–519, 1977.

Defant, A., Die absolute Topographie des physikalischen Meeresniveaus und der Druckflächen, sowie die Wasserbewegung des Atlantischen Ozeans, *Wiss. Ergeb. Dtsch. Atl. Exped. Meteor 1925–1927, 6*, 191–260, 1941.

Dietrich, G., K. Kalle, W. Krauss, and G. Siedler, *Allgemeine Meereskunde*, 3d ed., 593 pp., Bornträger, Berlin, 1975.

Emery, W. J., On the geographical variability of the upper level mean and eddy fields in the North Atlantic and North Pacific. *J. Phys. Oceanogr., 13*, 269–291, 1983.

Fiadeiro, M. E., and G. Veronis, On the determination of absolute velocities in the ocean, *J. Mar. Res., 40*, suppl., 159–182, 1982.

Fiadeiro, M. E., and G. Veronis, Circulation and heat flux in the Bermuda Triangle, *J. Phys. Oceanogr., 13*, 1158–1169, 1983.

Fofonoff, N. P., The Gulf Stream System, in *Evolution of Physical Oceanography*, edited by B. A. Warren and C. Wunsch, pp. 112–139, MIT Press, Cambridge, Mass., 1981.

Fofonoff, N. P., and R. M. Hendry, Current variability near the Southeast Newfoundland Ridge, *J. Phys. Oceanogr., 15*, 963–984, 1985.

Gould, W. J., Physical oceanography of the Azores front, *Prog. Oceanogr., 14*, 167–190, 1985.

Iselin, C. O. D., A study of the circulation of the western North Atlantic, *Pap. Phys. Oceanogr. Meteorol., 4*, 1–101, 1936.

Isemer, H.-J., and L. Hasse, *The Bunker Climate Atlas of the North Atlantic Ocean*, vol. 2, *Air-Sea Interactions*, 252 pp., Springer-Verlag, New York, 1985.

Käse, R. H., and G. Siedler, Meandering of the subtropical front southeast of the Azores, *Nature, 300*, 245–246, 1982.

Käse, R. H., W. Zenk, T. B. Sanford, and W. Hiller, Currents, fronts and eddy fluxes in the Canary Basin, *Prog. Oceanogr., 14*, 231–257, 1985.

Käse, R. H., J. F. Price, P. L. Richardson, and W. Zenk, A quasi-synoptic survey of the thermocline circulation and water mass distribution within the Canary Basin, *J. Geophys. Res., 91*, 9739–9748, 1986.

Krauss, W., The North Atlantic Current, *J. Geophys. Res., 91*, 5061–5074, 1986.

Krauss, W., and C. W. Böning, Lagrangian properties of eddy fields in the northern Atlantic as deduced from satellite-tracked buoys, *J. Mar. Res., 45*, 259–291, 1987.

Levitus, S., Climatological atlas of the world ocean, *NOAA Prof. Pap., 13*, 173 pp., 1982.

Maillard, C., *Atlas Hydrologique de l'Atlantique Nord-Est*, Institut Français de Recherche pour l'Exploitation de la Mer, Centre de Brest, Brest, France, 1986.

Mann, C. R., The termination of the Gulf Stream and the beginning of the North Atlantic current, *Deep Sea Res., 14*, 337–360, 1967.

Mountain, D. G., and J. L. Shuhy, Circulation near the Newfoundland Ridge, *J. Mar. Res., 38*(2), 205–213, 1980.

Olbers, D. J., M. Wenzel, and J. Willebrand, The inference of North Atlantic circulation patterns from climatological hydrographic data, *Rev. Geophys., 23*, 313–356, 1985.

Owens, W. B., A synoptic and statistical description of the Gulf Stream and the subtropical gyre using SOFAR floats, *J. Phys. Oceanogr., 14*, 104–113, 1984.

Richardson, P. L., Eddy kinetic energy in the North Atlantic from surface drifters, *J. Geophys. Res., 88*, 4355–4367, 1983.

Schmitz, W. J., Jr., SOFAR float trajectories associated with the Newfoundland Basin, *J. Mar. Res., 43*, 761–778, 1985.

Siedler, G., and L. Stramma, The applicability of the T/S method to geopotential anomaly computations in the northeast Atlantic, *Oceanol. Acta, 6*(2), 167–172, 1983.

Siedler, G., W. Zenk, and W. J. Emery, Strong current events related to a subtropical front in the northeast Atlantic, *J. Phys. Oceanogr., 15*, 885–897, 1985.

Stramma, L., Geostrophic transport in the Warm Water Sphere of the eastern subtropical North Atlantic, *J. Mar. Res., 42*, 537–558, 1984.

Stramma, L., and G. Siedler, Seasonal changes in the North Atlantic subtropical gyre, *J. Geophys. Res., 93*, 8111–8118, 1988.

Sy, A., Investigation of large-scale circulation patterns in the central North Atlantic: The North Atlantic Current, the Azores Current, and the Mediterranean Water plume in the area of the Mid-Atlantic Ridge, *Deep Sea Res., 35*, 383–413, 1988.

Worthington, L. V., Evidence for a two gyre circulation system in the North Atlantic, *Deep Sea Res., 9*, 51–67, 1962.

Worthington, L. V., On the North Atlantic circulation, *Johns Hopkins Stud. in Oceanogr., 6*, 110 pp., 1976.

Wüst, G., Schichtung und Zirkulation des Atlantischen Ozeans: Das Bodenwasser und die Stratosphäre, *Wiss. Ergeb. Dtsch. Atl. Exped. Meteor 1925–1927, 6*, 1–288, 1935.

B. Klein and G. Siedler, Institut für Meereskunde, Düsternbrooker Weg 20, D-2300 Kiel 1, Federal Republic of Germany.

(Received August 18, 1988;
revised December 20, 1988;
accepted October 10, 1988.)